

Commensurate Solid–Solid Phase Transitions in Self-Assembled Monolayers of Alkylthiolates Lying on Metal Surfaces

Y. Wang^{*,†,‡} J. G. Solano-Canchaya,[§] M. Alcamí,[†] H. F. Busnengo,[§] and F. Martín^{*,†,‡}

[†]Departamento de Química, Módulo 13, Universidad Autónoma de Madrid, 28049 Madrid, Spain

[‡]Instituto Madrileño de Estudios Avanzados en Nanociencia (IMDEA-Nanociencia), Cantoblanco, Madrid, Spain

[§]Instituto de Física Rosario (CONICET-UNR), Facultad de Ciencias Exactas, Ingeniería y Agrimensura, Universidad Nacional de Rosario, Avenida Pellegrini 250, 2000 Rosario, Argentina

S Supporting Information

ABSTRACT: A temperature-induced commensurate solid–solid phase transition in self-assembled monolayers (SAMs) of alkylthiolates lying on Pt(111) is predicted from molecular dynamics simulations based on ab initio potential energy surfaces. As the system cools down from room temperature to low enough temperature, SAMs of alkylthiolates with more than ~ 12 carbon atoms undergo an abrupt change of orientation from a nearly upright to a tilted configuration. As the initial hexagonal arrangement of the sulfur headgroups is kept fixed during the simulations, the phase transition is entirely governed by chain–chain interactions. Similar commensurate phase transitions are predicted for hexagonally arranged SAMs with lattice spacings of the order of 4.7–4.9 Å, which, among others, excludes the well-known cases of densely packed SAMs of alkylthiolates on Au(111) and Ag(111). These findings could be relevant for the design of novel electronic or optical devices controllable by temperature.

The self-assembled monolayers (SAMs) of alkylthiolates $S(CH_2)_{n-1}CH_3$ (hereafter C_n) on metal surfaces have been receiving widespread attention, owing to their important role in fundamental studies and versatile properties for technological applications.^{1–7} One interesting characteristic of these SAMs is their orientational structure on surfaces, which may affect electronic and optical properties and modify interactions with other interfaces. For instance, recent experiments⁸ have shown that the tilt of alkyl chains on oxide-free silicon enhances the electron transport efficiency and also that the structure of alkylthiolates on gold films can control the orientations of supported nematic liquid crystals.⁹

SAMs are paradigmatic examples of ordered 2D arrangements.^{1,2,5} Therefore, studies of phase transitions in reduced dimensionality have often considered these systems. The usual observation is that similar to bulk materials, SAMs “melt” at a high enough temperature, i.e., change from an ordered to a disordered phase. Melting has been thoroughly investigated in SAMs of alkylthiolates on Au(111).^{10–18} In particular, the variation of phase diagrams and melting curves with coverage and alkyl-chain length has revealed the important role of van der Waals chain–chain and covalent substrate–thiolate interactions.^{10,13,19} The former interaction is expected to play a dominant role for longer chain lengths n , while the latter is

more important for shorter n . For the longer chains, a solid–solid transition between commensurate and incommensurate phases has also been observed at temperatures close to melting,²⁰ thus showing that commensurability with the substrate is not a necessary condition for the existence of an ordered (solid-like) phase. To our knowledge, there is no evidence that SAMs of alkylthiolates can also undergo solid–solid (or order–order) phase transitions by preserving commensurability with the metal substrate. However, it is well-known that liquid crystal layers can exhibit such orientational phase transitions by changing temperature.^{21–24}

Earlier scanning probe microscopy²⁵ and low-energy electron diffraction (LEED)²⁶ experiments have established that on Au(111) surfaces, SAMs of alkylthiolates form a densely packed hexagonal arrangement with a nearest-neighbor sulfur–sulfur distance $d = 4.97$ Å. The structure formed by the sulfur heads corresponds to the so-called $(\sqrt{3} \times \sqrt{3})R30^\circ$ unit cell or its superstructure $c(4 \times 2)$ commensurate with gold lattice. Numerous experimental and theoretical studies (see ref 20 and therein) have shown that the alkyl chains are tilted away from the surface normal by about 30° . This tilt angle value on Au(111) does not vary significantly in a wide range of temperatures (e.g., from 4 K²⁷ up to RT).^{28,29} Formation of a disordered phase without diffusion of the sulfur headgroups (e.g., involving gauche defects and/or broad distribution of tilt angle of chains) depends on the chain length but generally occurs above RT. Alkylthiolate SAMs have also been found on other metal surfaces, such as Pt(111),^{30–34} Pd(111),³⁵ and Ag(111).^{36–39} They practically form the same densely packed hexagonal arrangement as on gold, although the corresponding lattice spacings d in the ML are quite different: $d = 4.97$, 4.80, and 4.42 Å for SAMs on gold, platinum, and silver, respectively.^{1,31} Since the experimental tilt angle for SAMs on Ag(111) is usually close to 0° ³⁶ (in some cases a value $\sim 10^\circ$ has been reported),^{36–39} it is widely accepted that the ML lattice spacing is the key parameter that determines the tilt angle of these full-coverage SAMs below the melting temperature. However, measurements and calculations of MLs characterized by intermediate lattice spacings are scarce and limited to only a few temperatures and chain lengths.^{33,34} Therefore, there is no definite information about the behavior

Received: June 15, 2012

Published: July 24, 2012

of SAMs on, e.g., Pt(111) and if the tilt angle value lies between the values observed on Au(111) and Ag(111).

We show that the way alkylthiolates self-assemble on Pt(111) is more complicated. We demonstrate that as the system cools down from RT (i.e., well below the melting point) to low enough temperature, SAMs of alkylthiolates with $> \sim 11$ C atoms undergo an orientational phase transition from a nearly upright to a tilted configuration by keeping the hexagonal arrangement of the anchoring points (as schematically illustrated in the insets of Figure 2a). In other words, SAMs on Pt(111) experience commensurate solid–solid phase transitions. The critical temperature for these transitions strongly depends on chain length. Similar phase transitions are not observed on Au(111) and Ag(111), in agreement with experiments.

We have performed large-scale constant-temperature MD simulations by using the DL_POLY 2 package⁴⁰ and a newly parametrized force field based on high-level ab initio computations for the noncovalent interactions among alkylthiolate molecules.⁴¹ The appropriateness of the force field has been established in previous work.⁴¹ To reduce the computational cost of the MD simulations, we make use of rigid all-trans chain approximation, i.e., gauche defects are not considered, which has been suggested as a reasonable approximation below RT.⁴² To prove this in our work, we have explicitly included bending and rotation of the S–C and C–C bonds in a few representative cases [see Supporting Information (SI)]. The values of the tilt angles obtained from the latter calculations typically differ by $< 5^\circ$ from those obtained within the rigid chain approximation. The interaction between the alkyl chains and the metal substrate is neglected, which is a reasonable approximation to describe SAMs of long-chain thiolates.⁴³ We utilize a rather large 20×20 unit cell comprising 400 molecules whose sulfur heads have been fixed forming the hexagonal arrangement observed on Au(111), Pt(111), or Ag(111). We have checked convergence of our results by performing explicit calculations for the series of unit cells 8×8 , 10×10 , 16×16 , and 20×20 (see SI). We have used the Berendsen thermostat, where the instantaneous temperature is pushed toward the desired temperature by scaling the velocities at each step and a time step of 0.5 fs.

The reliability of MD simulations is confirmed by comparing our results with experiments for SAMs on Au(111), which have been extensively investigated and are the benchmark in this field.^{10,27–29,44,45} As can be seen in Figure 1, good agreement between simulated and experimental tilt angles^{10,27–29,44,45} is

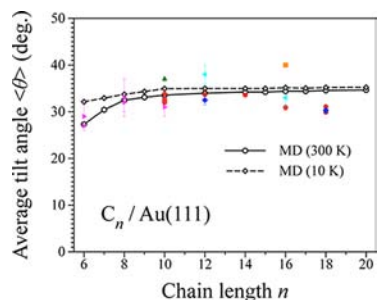


Figure 1. Comparison between theoretical and experimental average tilt angles for C_n SAMs on the Au(111) surface. Experimental measurements around RT are indicated by solid circles,²⁹ diamonds,¹⁰ squares,⁴⁴ and triangles²⁸ and left triangles.⁴⁵ Solid right triangles indicate measurements at 4 K.²⁷

obtained for a variety of sizes ranging from C_6 to C_{20} . Both theory and various experiments predict a tilt angle value of $\sim 30^\circ$ at RT. This value is more or less the same for all thiolates with $n \geq 10$. The results show that except for very short chains, the tilt angle barely changes with temperature (provided it is smaller than the melting temperature, ~ 350 K).^{14,46}

To explore phase transition of SAMs on Pt(111), MD simulations were performed at various temperatures from 300 to 10 K. The tilt angle θ , averaged over 100 ps after MD equilibrium, demonstrates an abrupt jump at a certain critical temperature T_c , depending on the chain length n of the alkylthiolate C_n . For instance, the C_{16} molecular chains are aligned almost perpendicular to the Pt(111) substrate ($\theta \sim 2^\circ$) at RT. Surprisingly, when the temperature decreases from 250 to 240 K, the tilt angle increases from 2° to $\sim 20^\circ$ (see Figure 2a), indicating an unambiguous phase change from upright to

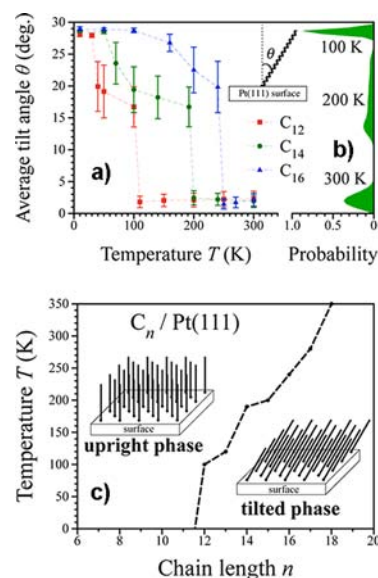


Figure 2. (a) Average tilt angle, θ , as a function of temperature T for SAMs of C_{12} , C_{14} , and C_{16} on Pt(111). Bars indicate standard deviation with respect to mean value. (b) Distribution of tilt angles at various temperatures for C_{16} on Pt(111). (c) (T, n) phase diagram for a $(\sqrt{3} \times \sqrt{3})R30^\circ$ SAM of alkylthiolate C_n on Pt(111) surface.

tilted orientation. Further cooling down from this critical temperature ($T_c \approx 240$ K) gradually increases the tilt angle; below 100 K, it remains almost constant ($\theta \approx 30^\circ$). A more detailed information is obtained by analyzing the distribution of tilt angles at different temperatures. As illustrated by bars superimposed to different points in Figure 2a, the distribution of tilt angles is narrow (within $\pm 1^\circ$) at very low ($T < 100$ K) or high ($T > 250$ K) temperatures, while this distribution remarkably spreads out at intermediate temperatures (e.g., standard deviation at 240 K is $\pm 4^\circ$). This implies an intermediate state where the alkylthiolate SAMs evolve from one to another well-ordered phase. The variation of the tilt-angle distribution with temperature is shown in Figure 2b for SAMs of C_{16} .

Similar phase transitions occur in the SAMs of C_{12} and C_{14} except that the critical temperature is different, $T_c \approx 200$ and 100 K for C_{12} and C_{14} , respectively, as shown in Figure 2a. By relating the critical temperature T_c to the chain length n , one obtains a (T, n) phase diagram as that shown in Figure 2c for C_n SAMs on Pt(111). We can see that the T_c increases as the

thiolate chain becomes longer. For alkylthiolates longer than C_{18} , however, the T_c is expected to probably exceed the melting temperature of SAMs (about 350 K).^{14,46} On the other hand, no phase transition occurs at any temperature for alkyl chains shorter than C_{12} . Therefore, the present theory predicts that on Pt(111), this solid–solid phase transition can only be observed for SAMs of alkylthiolates with intermediate chain length (C_{12} – C_{18}).

Now, one may raise the following question. Why is such a phase transition for alkylthiolate SAMs not observed on Au(111) or Ag(111) surfaces? To answer this, we propose a simple single-chain model.^{41,43} This model describes the two-dimensional periodic SAM by using a hexagonal unit cell containing only one alkylthiolate molecule, which is allowed to tilt, rotate, and twist around a fixed headgroup position. To mimic different substrates, we select the lattice parameter value (i.e., distance between nearest-neighbor sulfur headgroups) to be 4.97, 4.80, and 4.42 Å for Au(111), Pt(111), and Ag(111), respectively. From the corresponding 3D potential energy surface, we have evaluated the minimum-energy path U and the entropy along the tilt-angle coordinate θ (see SI).^{41,43} Figure 3a

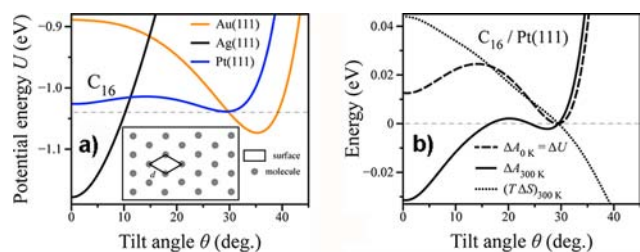


Figure 3. (a) Potential energy per molecule U as a function of tilt angle for SAMs on different surfaces, based on the simple model described in the text. Unit cell of the SAM on the metal surface used in model is also schematically illustrated. (b) Same as (a) but with free energy A at 0 and 300 K and entropic contribution $T\Delta S$ at 300 K. ΔU , ΔS , and ΔA are their respective values at minimum of U .

depicts the U – θ curves for C_{16} SAMs on gold, silver, and platinum surfaces. One can see that the U – θ curve for Au(111) has a minimum at $\sim 30^\circ$, in reasonable agreement with the experimental value of the average tilt angle at RT. In the case of the Ag(111) surface, the minimum of the U – θ curve appears close to zero, which also agrees with the fact that the tilt angles are much smaller on silver than on gold. Figure 3b shows the variations of entropy S and free energy A with tilt angle for the 3D model describing C_{16} SAMs on platinum. As can be seen, the entropic contribution to free energy decreases monotonously with θ . Thus, at 300 K, the minimum of the free energy appears at 0° instead of at 30° . Consequently, the tilt angle must drop from $\sim 30^\circ$ to $\sim 0^\circ$ when heating up from 0 K to RT. This dramatic change of the free-energy with temperature on Pt(111) is possible because the two minima in the U – θ curve have similar depth and are separated by only 0.02 eV (or ~ 200 K). As the chain length becomes shorter, the energy barrier between the two minima becomes lower, which explains the decrease of T_c when the chain is shorter.

Similar S – θ and A – θ plots (see SI) explain why there is not such a phase transition on Au(111) and Ag(111): The increase of the entropic contribution that results from increasing the tilt angle from 0° to 30° does not lead to a significant change of the free-energy minimum position. This is consistent with previous studies, which have reported a relatively small variation of the

tilt angle with temperature for SAMs of alkylthiolates on Au(111)^{42,47} and Ag(111).

For platinum the temperature-induced phase transition only takes place for SAMs within a given range of n . This can be understood with the help of the above simple model. Figure 4a

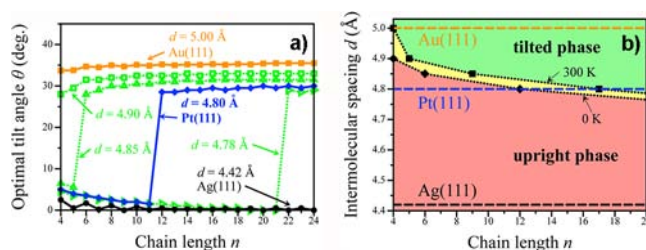


Figure 4. (a) Optimal tilt angle as a function of chain length for various intermolecular spacings d , based on the simple model described in the text. (b) (d, n) phase diagram obtained from MD calculations at 0 and 300 K. Yellow area shows where phase transition is expected below RT.

shows the the tilt angle value corresponding to the global minimum of the 3D potential energy surface as a function of n for various d . As the potential energy surface minimum does not contain any information about temperature, the plotted values of the tilt angle should only be compared with measurements and calculations performed at 0 K. However, the information contained in this figure is still valid for qualitative interpretations at $T > 0$ K. As seen, the model predicts that the tilt angle should remain almost invariant with chain length for Au(111), agreeing with previous works and present MD calculations. The same is true for Ag(111). In contrast, for Pt(111), there is an abrupt jump in the the tilt angle value for $n = 12$. On Pt(111), SAMs with shorter chains ($n < 12$) behave like those on Ag(111), whereas SAMs with longer chains ($n > 12$) behave like those on Au(111). This is in qualitative agreement with results of more involved MD calculations at 300 K. Therefore for temperatures significantly above 0 K, phase transitions should only occur for SAMs of alkylthiolates in a narrow n range. It is interesting to note that although the present single-chain model forces all alkylthiolates to move synchronously, the critical size n_c at which the abrupt jump is observed, $n_c = 12$, is close to the n values where phase transitions are actually observed on Pt(111).

Figure 4a shows that for other d close to that of SAMs of alkylthiolates on Pt(111), similar “jumps” in the tilt angle are obtained at specific n . In particular, critical chain lengths appear at $n = 6$ and 22 for $d = 4.85$ and 4.78 Å, respectively. Hence, critical chain length is very sensitive to lattice spacing. As shown in Figure 4a, a slight decrease in lattice spacing from 4.80 to 4.78 Å leads to a significant increase of critical chain length from 12 to 22.

Based on these findings, one can build a (d, n_c) phase diagram as shown in Figure 4b for temperatures of 0 and 300 K (from MD simulations). The diagram shows that temperature-induced commensurate solid–solid phase transitions in SAMs of alkylthiolates can only take place for n and d lying between two boundary lines corresponding to 300 and 0 K (yellow area, Figure 4b). Apart from confirming again that no commensurate solid–solid phase transition can occur on Au(111) or Ag(111) for any n and that such a phase transition is only possible on Pt(111) in a narrow n value range ($n = 12$ – 17), the diagram shows that phase transitions are also possible in a finite range of

n for SAMs of alkylthiolates with lattice spacing between 4.7 and 4.9 Å.

In summary, a temperature-induced commensurate solid–solid orientational phase transition of 2D SAMs of alkylthiolates has been found as a result of MD simulations carried out by using a force field based on high-level ab initio calculations. The phase transition is entirely governed by chain–chain interactions. The key parameters are the SAM lattice spacing and the molecular chain length. For hexagonally arranged SAMs on Pt(111), such phase transitions occur below RT for alkylthiolates with 12–18 carbon atoms. Similar commensurate phase transitions are expected to occur in hexagonally arranged SAMs with lattice spacings between 4.7 and 4.9 Å, irrespective of the nature of the substrate. Building up systems with the appropriate lattice spacings to observe such phase transitions should be possible by introducing proper functional groups and/or choosing proper supporting substrates. This could be relevant in the design of novel electronic or optical devices controllable by temperature.

■ ASSOCIATED CONTENT

● Supporting Information

This material is available free of charge via the Internet at <http://pubs.acs.org/>.

■ AUTHOR INFORMATION

Corresponding Author

yang.wang@uam.es; fernando.martin@uam.es

Notes

The authors declare no competing financial interest.

■ ACKNOWLEDGMENTS

We thank the CCC-UAM and the RES for allocation of computer time. Work partially supported by projects FIS2010-15127, CTQ2010-17006, and CSD2007-00010 (MICINN), S2009/MAT1726 (CAM), A2/039631/11 (AECID), PIP 0667 (CONICET), and PICT Bicentenario 1962 (ANPCyT).

■ REFERENCES

- (1) Ulman, A. *Chem. Rev.* **1996**, *96*, 1533.
- (2) Schreiber, F. *Prog. Surf. Sci.* **2000**, *65*, 151.
- (3) Love, J. C.; Wolfe, D. B.; Chabinyc, M. L.; Paul, K. E.; Whitesides, G. M. *J. Am. Chem. Soc.* **2002**, *124*, 1576.
- (4) Schreiber, F. *J. Phys.: Condens. Matter* **2004**, *16*, R881.
- (5) Love, J. C.; Estroff, L. A.; Kriebel, J. K.; Nuzzo, R. G.; Whitesides, G. M. *Chem. Rev.* **2005**, *105*, 1103.
- (6) Vericat, C.; Vela, M. E.; Salvarezza, R. C. *Phys. Chem. Chem. Phys.* **2005**, *7*, 3258.
- (7) Chu, C.; Na, J. S.; Parsons, G. N. *J. Am. Chem. Soc.* **2007**, *129*, 2287.
- (8) Shpaisman, H.; Seitz, O.; Yaffe, O.; Roodenko, K.; Scheres, L.; Zuilhof, H.; Chabal, Y. J.; Sueyoshi, T.; Kera, S.; Ueno, N.; Vilan, A.; Cahen, D. *Chem. Sci.* **2012**, *3*, 851.
- (9) Gupta, V. K.; Abbott, N. L. *Science* **1997**, *276*, 1533.
- (10) Fenter, P.; Eisenberger, P.; Liang, K. S. *Phys. Rev. Lett.* **1993**, *70*, 2447.
- (11) Badia, A.; Lennox, R. B.; Back, R. *Angew. Chem., Int. Ed.* **1994**, *33*, 2332.
- (12) Delamarche, E.; Michel, B.; Kang, H.; Gerber, C. *Langmuir* **1994**, *10*, 4103.
- (13) Badia, A.; Singh, S.; Demers, L.; Cuccia, L.; Brown, G. R.; Lennox, R. B. *Chem.—Eur. J.* **1996**, *2*, 359.
- (14) Bensebaa, F.; Ellis, T. H.; Badia, A.; Lennox, R. B. *Langmuir* **1998**, *14*, 2361.
- (15) Poirier, G. E.; Fitts, W. P.; White, J. M. *Langmuir* **2001**, *17*, 1176.
- (16) Qian, Y.; Yang, G.; Yu, J.; Jung, T. A.; Yu Liu, G. *Langmuir* **2003**, *19*, 6056.
- (17) Schreiber, F.; Gerstenberg, M. C.; Dosch, H.; Scoles, G. *Langmuir* **2003**, *19*, 10004.
- (18) Zhang, Z. S.; Wilson, O. M.; Efremov, M. Y.; Olson, E. A.; Braun, P. V.; Senaratne, W.; Ober, C. K.; Zhang, M.; Allen, L. H. *Appl. Phys. Lett.* **2004**, *84*, 5198.
- (19) Barrena, E.; Palacios-Lidón, E.; Munuera, C.; Torrelles, X.; Ferrer, S.; Jonas, U.; Salmeron, M.; Ocal, C. *J. Am. Chem. Soc.* **2004**, *126*, 385.
- (20) Fenter, P. In *Thin Films*; Ulman, A., Ed.; Academic Press: San Diego, 1998; Vol. 24; Chapter Self-assembled monolayers of thiols.
- (21) Sonin, A.; Yethiraj, A.; Bechhoefer, J.; Frisken, B. *Phys. Rev. B* **1995**, *52*, 6260.
- (22) Khazimullin, M. V.; Krekhov, A. P.; Lebedev, Y. A.; Scaldin, O. A. *Tech. Phys. Lett.* **1997**, *23*, 341.
- (23) Genzer, J.; Sivaniah, E.; Kramer, E. J.; Wang, J.; Körner, H.; Char, K.; Ober, C. K.; DeKoven, B. M.; Bubeck, R. A.; Fischer, D. A.; Sambasivan, S. *Langmuir* **2000**, *16*, 1993.
- (24) Barbero, G.; Komitov, L. *J. Appl. Phys.* **2009**, *105*, 064516.
- (25) Chidsey, C. E.; Loiacono, D. N. *Langmuir* **1990**, *6*, 682.
- (26) Strong, L. *Langmuir* **1988**, *4*, 546.
- (27) Han, P.; Kurlanda, A. R.; Giordano, A. N.; Nanayakkara, S. U.; Blake, M. M.; Pochas, C. M.; Weiss, P. S. *ACS Nano* **2009**, *3*, 3115.
- (28) Fenter, P.; Eberhardt, A.; Eisenberger, P. *Science* **1994**, *266*, 1216.
- (29) Fenter, P.; Eberhardt, A.; Liang, K. S.; Eisenberger, P. *J. Chem. Phys.* **1997**, *106*, 1600.
- (30) Kim, S. S.; Kim, Y.; Kim, H. I.; Lee, S. H.; Lee, T. R.; Perry, S. S.; Rabalais, J. W. *J. Chem. Phys.* **1998**, *109*, 9574.
- (31) Yang, Y.; Yen, Y.; Ou Yang, L.; Yau, S.; Itaya, K. *Langmuir* **2004**, *20*, 10030.
- (32) Addato, M. A. F.; Rubert, A. A.; Bentez, G. A.; Fonticelli, M. H.; Carrasco, J.; Carro, P.; Salvarezza, R. C. *J. Phys. Chem. C* **2011**, *115*, 17788.
- (33) Petrovykh, D. Y.; Kimura-Suda, H.; Opdahl, A.; Richter, L. J.; Tarlov, M. J.; Whitman, L. J. *Langmuir* **2006**, *22*, 2578.
- (34) Li, Z.; Chang, S.-C.; Williams, R. S. *Langmuir* **2003**, *19*, 6744.
- (35) Love, J.; Wolfe, D.; Haasch, R.; Chabinyc, M.; Paul, K.; Whitesides, G.; Nuzzo, R. *J. Am. Chem. Soc.* **2003**, *125*, 2597.
- (36) Ehler, T. T.; Malmberg, N.; Noe, L. J. *J. Phys. Chem. B* **1997**, *101*, 1268.
- (37) Bryant, M. A.; Pemberton, J. E. *J. Am. Chem. Soc.* **1991**, *113*, 3629.
- (38) Walczak, M. M.; Chung, C.; Stole, S. M.; Widrig, C. A.; Porter, M. D. *J. Am. Chem. Soc.* **1991**, *113*, 2370.
- (39) Laibinis, P. E.; Whitesides, G. M.; Allara, D. L.; Tao, Y.-T.; Parikh, A. N.; Nuzzo, R. G. *J. Am. Chem. Soc.* **1991**, *113*, 7152.
- (40) Smith, W.; Forester, T.; Todorov, I.; Leslie, M. *the DL_Poly 2 User Manual*; CCLRC Daresbury Laboratory: Daresbury, U.K., 2006.
- (41) Canchaya, J. S.; Wang, Y.; Alcamí, M.; Martín, F.; Busnengo, H. *Phys. Chem. Chem. Phys.* **2010**, *12*, 7555.
- (42) Vemparala, S.; Karki, B. B.; Kalia, R. K.; Nakano, A.; Vashishta, P. *J. Chem. Phys.* **2004**, *121*, 4323.
- (43) Abufager, P.; Canchaya, J. S.; Wang, Y.; Alcamí, M.; Martín, F.; Soria, L. A.; Martiarena, M.; Reuter, K.; Busnengo, H. *Phys. Chem. Chem. Phys.* **2011**, *13*, 9353.
- (44) Nuzzo, R.; Dubois, L.; Allara, D. *J. Am. Chem. Soc.* **1990**, *112*, 558.
- (45) Fischer, D.; Marti, A.; Hähner, G. *J. Vac. Sci. Technol. A* **1997**, *15*, 2173.
- (46) Venkataraman, M.; Pradeep, T. *Anal. Chem.* **2000**, *72*, 5852.
- (47) Hautman, J.; Klein, M. L. *J. Chem. Phys.* **1990**, *93*, 7483.